Asian Journal of Chemistry; Vol. 38, No. 9 (2026), 2438-2446
ASIAN JOURNAL OF CHEMISTRY
https://doi.org/10.14233/ajchem.2026.36375

Synthesis of New Indole-Pyrazole linked Isoxazoles as Potent Antibacterial and Antibiofilm Agents

VENKATESH REDDYCHERLA[1,2,*], K. CHENNAKESAVULU[1,*], G. RAMANJANEYA REDDY[1] and R. BHASKAR REDDY[1]

[1]Department of Chemistry, Sathyabama Institute of Science and Technology (Deemed University), Jeppiaar Nagar, Chennai-600119, India
[2]Center for Nanoscience and Nanotechnology, Sathyabama Institute of Science and Technology (Deemed University), Jeppiaar Nagar, Chennai-600119, India

*Corresponding authors: E-mail: venkateshtsp@gmail.com; chennanml@yahoo.com

Received: 6 May 2026 *Accepted*: 14 August 2026 *Published online*: 5 September 2026 AJC-22472

A series of new indole-pyrazole-linked isoxazole hybrids (**5a-o**) were synthesized using Cu(I)-catalyzed 1,3-dipolar cycloaddition and assessed for antibacterial and antibiofilm activities against methicillin-sensitive *Staphylococcus aureus* (MSSA), methicillin-resistant *Staphylococcus aureus* (MRSA) and vancomycin-resistant *Staphylococcus aureus* (VRSA) pathogens. Biological evaluation showed that the dihalogenated derivatives, particularly 3,5-dichloro (**5g**) and 2,4-dichloro (**5i**), exhibited pronounced antibacterial activity comparable to dicloxacillin. Both compounds substantially inhibited biofilm formation. Molecular docking studies against penicillin-binding protein (PDB ID: 1MWT) supported the experimental findings, with favourable binding interactions and high predicted affinity. Structure-activity relationship analysis indicated that dichloro substitution enhanced antibacterial potency. These hybrid compounds may serve as potential candidates for further investigation against resistant *Staphylococcus aureus* infections.

Keywords: Antibacterial, Biofilm, Indole, Isoxazoles, Pyrazole, Molecular docking.

INTRODUCTION

Indole, pyrazole and isoxazole are established heterocyclic scaffolds in medicinal chemistry and provide diverse structural frameworks for the development of biologically active molecules [1-6]. Isoxazole derivatives have been investigated extensively as pharmacologically relevant compounds and synthetic intermediates, including in the preparation of β-lactam antibiotics such as cloxacillin and dicloxacillin [7]. The pyrazole ring is widely incorporated into organic, bioorganic and medicinal compounds due of its accessible synthesis and broad biological activity [3,4]. Indole derivatives have likewise attracted attention for their antibacterial activity against clinically relevant pathogens, including methicillin-resistant *Staphylococcus aureus* (MRSA) [8]. Indole containing hybrids have been reported to exhibit activity against a range of pathogenic and drug-resistant bacterial strains [9-14].

This investigation is relevant to the continuing increase in multidrug resistance (MDR), which presents a major challenge in the treatment of bacterial infections and contributes substantially to infection-associated mortality [15]. *S. aureus* is an opportunistic pathogen and a common component of the human microbiota, with asymptomatic nasal or skin colonization occurring in approximately one-third of the population [16]. Following disruption of epithelial barriers, *S. aureus* can cause infections involving multiple tissues and organs. Its capacity to adapt to host environments and antimicrobial pressure contributes to its clinical importance [17]. Methicillin-susceptible *S. aureus* (MSSA), methicillin-resistant *S. aureus* (MRSA) and vancomycin-resistant *S. aureus* (VRSA) represent clinically important phenotypes associated with antimicrobial resistance [18,19]. The continuing emergence of resistant strains has increased the need for antibacterial compounds with new chemical scaffolds and mechanisms of action [20-22].

Biofilm formation further complicates the management of *S. aureus* infections. Biofilms are structured bacterial communities associated with persistent infections in humans and animals and with contamination of medical implants and healthcare equipment [23]. Bacterial aggregation precedes biofilm maturation [24], while the resulting extracellular matrix and altered physiological state can reduce susceptibility to antimicrobial treatment [25,26]. Biofilm-associated *S. aureus* infections are consequently difficult to eradicate and represent an important therapeutic problem [27].

Molecular hybridization, in which two or more biologically relevant pharmacophores are combined within one molecular framework, provides a rational approach to the design of new antibacterial compounds [28-30]. On this basis, new indole–pyrazole-linked isoxazoles were designed and synthesized by a Cu-catalyzed 1,3-dipolar cycloaddition involving an alkyne and substituted aryl aldehyde-derived precursors. The resulting compounds were evaluated for antibacterial activity against selected strains of *S. aureus*. The incorporation of three heterocyclic units within a single molecular framework was designed to assess their influence on antibacterial activity and biofilm inhibition. Moreover, the molecular design was based on a molecular hybridization technique targeted at increasing EGFR inhibitory activity and antiproliferative efficacy (Fig. 1).

EXPERIMENTAL

All reagents were of analytical grade or chemically pure. Analytical thin-layer chromatography was performed on silica gel 60 F_{254} plates (Merck). ^{1}H NMR spectra were acquired using a Varian Gemini 400 MHz spectrometer. ^{13}C NMR spectra were obtained using a Bruker 100 MHz spectrometer. Chemical shift measurements were quantified in parts per million (ppm, δ), with tetramethylsilane serving as an internal reference. Mass spectrometry measurements were performed using the electron impact (EI) method.

Synthesis of (*E*)-5-methyl-4-((1-methyl-1*H*-indol-3-yl)-methylene)-2-(prop-2-yn-1-yl)-2,4-dihydro-3*H*-pyrazol-3-one (4): A mixture of 1-methyl-1*H*-indole-3-carbaldehyde (**1**, 3 g, 0.019 mol), 5-methyl-2-(prop-2-yn-1-yl)-2,4-dihydro-3*H*-pyrazol-3-one (**3**, 2.6 g, 0.019 mol) and piperidene (0.003 mol) was refluxed in methanol for 16 h. Then, the reaction mixture was allowed to cool to room temperature for a period of 2 h. The precipitate formed was filtered, washed with cold ethanol and dried. In the final step, the crude solid was crystallized with ethanol, resulting in a pale red solid with a yield of 69%. ^{1}H NMR (400 MHz, DMSO-d_6, δ ppm): 7.79 (s, 1H), 7.66 (d, J = 8.0 Hz, 1H), 7.41 (d, J = 8.0 Hz, 1H), 7.19-7.16

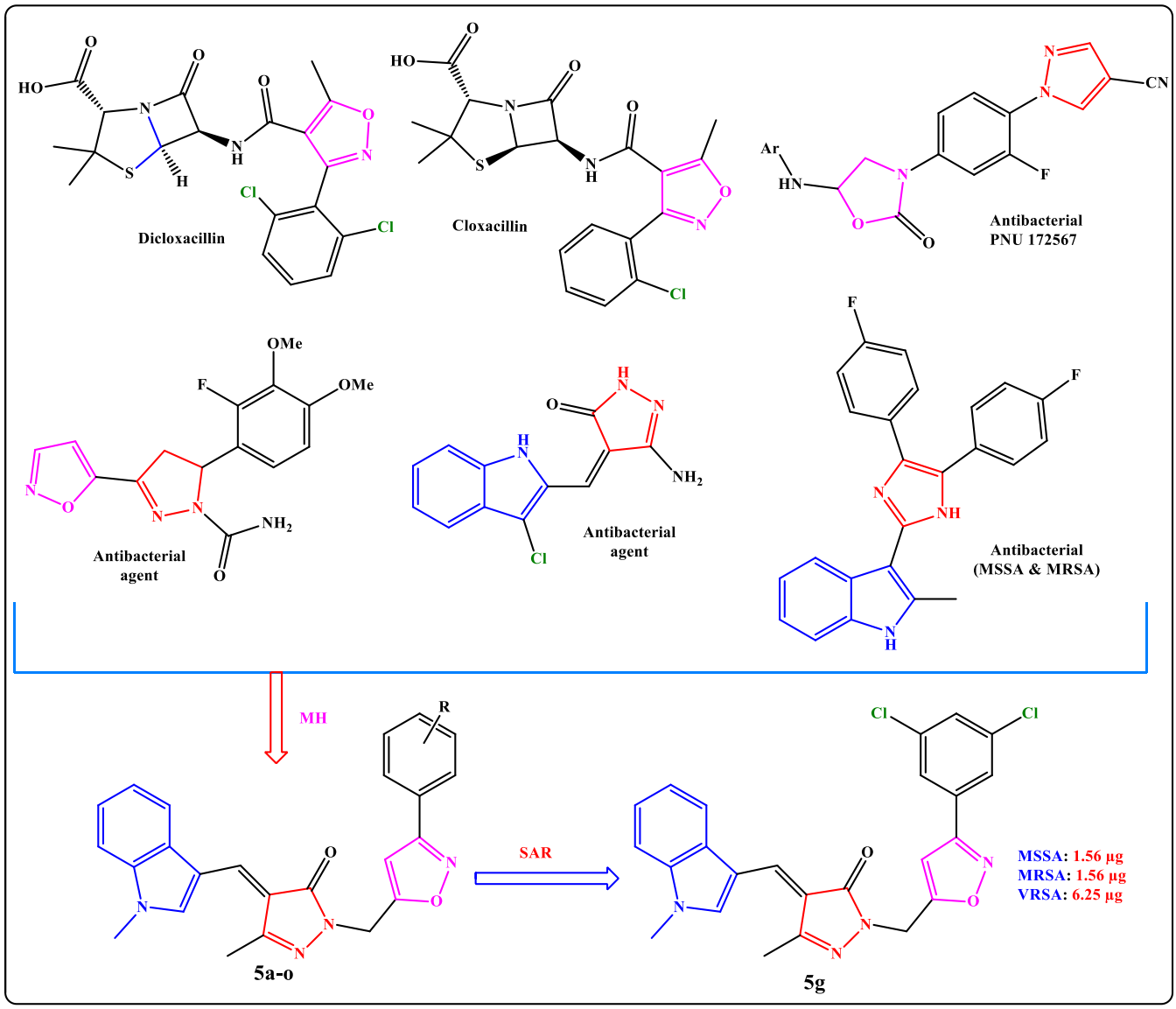

Fig. 1. Design strategy for the synthesis of indole-pyrazole linked Isoxazoles *via* a molecular hybridization approach

(m, 1H), 7.09 (s, 1H), 7.04-7.02 (m, 1H), 3.93 (d, *J* = 4.0 Hz, 2H, N-CH_2), 3.53 (s, 3H, N-CH_3), 2.68 (s, 3H, -CH_3), 1.96 (t, *J* = 4.0 Hz, 1H, CH). ESI-MS: 278 [M + H].

Synthesis of (*E*)-2-((3-(aryl)isoxazol-5-yl)methyl)-5-methyl-4-((1-methyl-1*H*-indol-3-yl)methylene)-2,4-dihydro-3*H*-pyrazol-3-one (5a-o): Aldehyde (0.32 g, 0.003 mol) was added to a solution of hydroxylamine hydrochloride (0.22 g, 0.0033 mol) in 10 mL of 1:1 *t*-BuOH:H_2O mixture. Subsequently, NaOH (0.13 g, 0.0033 mol) was introduced and after 30 min of agitation at room temperature, TLC analysis verified the completion of oxime synthesis. Chloramine-T trihydrate (0.9 g, 0.0033 mol) was gradually added over 10 min, followed by CuI (44 mg, 0.233 mmol). Compound **4** (0.4 g, 0.002 mol) was added, the pH was adjusted to 6 with a few drops of 1 M NaOH and stirring was continued for an additional 8-10 h. The reaction mixture was added to 50 mL of cold water, followed by the addition of 10 mL of dilute NH_4OH to remove any copper salts (**Scheme-I**). The crude was refined using column chromatography with silica gel and a liquid combination of 25% ethyl acetate and hexane.

(*E*)-5-Methyl-4-((1-methyl-1*H*-indol-3-yl)methylene)-2-((3-phenylisoxazol-5-yl)methyl)-2,4-dihydro-3*H*-pyrazol-3-one (5a): Yield: 65%; m.p.: 147-149 ºC; ^{1}H NMR (400 MHz, DMSO-d_6, δ ppm): 7.78 (s, 1H), 7.68 (d, *J* = 8.0 Hz, 1H), 7.55 (d, *J* = 8.0 Hz, 2H), 7.42 (d, *J* = 8.0 Hz, 1H), 7.34-7.31 (m, 3H), 7.18-7.15 (m, 1H), 7.09 (s, 1H), 7.03-7.01 (m, 1H), 6.83 (s, 1H, isoxazole), 5.10 (s, 2H, N-CH_2), 3.54 (s, 3H, N-CH_3), 2.64 (s, 3H, -CH_3); ^{13}C NMR (100 MHz, DMSO-d_6, δ ppm): 169.47, 163.47, 160.31, 154.52, 138.41, 133.38, 132.03, 130.79, 129.95, 128.83, 128.39 (2C), 127.67 (2C), 124.57, 123.74, 122.38, 121.26, 117.87, 110.46, 99.69, 44.20, 36.37, 14.53; ESI-MS: calcd. for $C_{24}H_{20}N_4O_2$: $[M]^+$ *m/z*: 396, found: 397 $[M+H]^+$. Anal. calcd. (found) % for $C_{24}H_{20}N_4O_2$: C, 72.71 (72.73); H, 5.09 (5.05); N, 14.13 (14.11).

(*E*)-5-Methyl-4-((1-methyl-1*H*-indol-3-yl)methylene)-2-((3-(*p*-tolyl)isoxazol-5-yl)methyl)-2,4-dihydro-3*H*-pyrazol-3-one (5b): Yield: 65%; m.p.: 151-153 ºC; ^{1}H NMR (400 MHz, DMSO-d_6, δ ppm): 7.79 (s, 1H), 7.66 (d, *J* = 8.0 Hz, 1H), 7.51 (d, *J* = 8.0 Hz, 2H), 7.42 (d, *J* = 8.0 Hz, 1H), 7.32 (d, *J* = 8.0 Hz, 2H), 7.18-7.16 (m, 1H), 7.07 (s, 1H), 7.04-7.01 (m, 1H), 6.84 (s, 1H, isoxazole), 5.11 (s, 2H, N-CH_2), 3.53 (s, 3H, N-CH_3), 2.65 (s, 3H, -CH_3), 2.25 (s, 3H, -CH_3); ^{13}C NMR (100 MHz, DMSO-d_6, δ ppm): 169.50, 163.62, 160.47, 154.52, 139.36, 138.42, 133.35, 132.17, 130.52, 129.15 (2C), 128.13, 127.12 (2C), 124.81, 123.60, 122.41, 121.44, 117.55, 110.53, 99.81, 44.28, 36.31, 21.56, 14.35; ESI-MS: calcd. for $C_{25}H_{22}N_4O_2$: $[M]^+$ *m/z*: 410, found: 411 $[M+H]^+$. Anal. calcd. (found) % for $C_{25}H_{22}N_4O_2$: C, 73.15 (73.19); H, 5.40 (5.43); N, 13.65 (13.62).

(*E*)-2-((3-(3,5-Dimethylphenyl)isoxazol-5-yl)methyl)-5-methyl-4-((1-methyl-1*H*-indol-3-yl)methylene)-2,4-dihydro-3*H*-pyrazol-3-one (5c): Yield: 50%; m.p.: 158-161 ºC; ^{1}H NMR (400 MHz, DMSO-d_6, δ ppm): 7.80 (s, 1H), 7.66 (d, *J* = 8.0 Hz, 1H), 7.52 (s, 2H), 7.43 (d, *J* = 8.0 Hz, 1H), 7.19-7.17 (m, 1H), 7.13 (s, 1H), 7.07 (s, 1H), 7.04-7.01 (m, 1H), 6.84 (s, 1H, isoxazole), 5.10 (s, 2H, N-CH_2), 3.53 (s, 3H, N-CH_3), 2.64 (s, 3H, -CH_3), 2.16 (s, 6H, 2-CH_3); ^{13}C NMR (100 MHz, DMSO-d_6, δ ppm): 169.26, 163.75, 160.49, 154.46, 138.81, 137.50 (2C), 133.71, 132.58, 132.05, 131.04, 128.27, 126.14 (2C), 124.53, 123.30, 122.54, 121.44, 117.76, 110.52, 99.76, 44.30, 36.23, 20.31 (2C), 14.47; ESI-MS: calcd. for $C_{26}H_{24}N_4O_2$: $[M]^+$ *m/z*: 424, found: 425 $[M+H]^+$. Anal. calcd. for $C_{26}H_{24}N_4O_2$: C, 73.56; H, 5.70; N, 13.20. Found: C, 73.59; H, 5.73; N, 13.17.

(*E*)-2-((3-(4-Methoxyphenyl)isoxazol-5-yl)methyl)-5-methyl-4-((1-methyl-1*H*-indol-3-yl)methylene)-2,4-dihydro-3*H*-pyrazol-3-one (5d): Yield: 40%; m.p.: 163-165 ºC; ^{1}H NMR (400 MHz, DMSO-d_6, δ ppm): 7.79 (s, 1H), 7.02-7.67 (m, 3H), 7.43 (d, *J* = 8.0 Hz, 1H), 7.19-7.16 (m, 1H), 7.08 (s, 1H), 7.05-7.02 (m, 1H), 6.98 (d, *J* = 8.0 Hz, 2H), 6.84 (s, 1H, isoxazole), 5.10 (s, 2H, N-CH_2), 3.84 (s, 3H, OCH_3), 3.54 (s, 3H, N-CH_3), 2.65 (s, 3H, -CH_3); ^{13}C NMR (100 MHz, DMSO-d_6, δ ppm): 169.44, 163.49, 160.68, 159.34, 154.30, 138.66, 133.18, 132.24, 129.34 (2C), 128.73, 124.32, 123.28, 122.46, 121.31, 120.44, 117.42, 114.57 (2C), 110.44, 99.82, 56.23, 44.52, 36.44, 14.65; ESI-MS: calcd. for $C_{25}H_{22}N_4O_3$: $[M]^+$ *m/z*: 426, found: 427 $[M+H]^+$. Anal. calcd. (found) % for $C_{25}H_{22}N_4O_3$: C, 70.41 (70.43); H, 5.20 (5.16); N, 13.14 (13.11).

((*E*)-2-((3-(3,5-Dimethoxyphenyl)isoxazol-5-yl)methyl)-5-methyl-4-((1-methyl-1*H*-indol-3-yl)methylene)-2,4-dihydro-3*H*-pyrazol-3-one (5e): Yield: 30%; m.p.: 170-172 ºC; ^{1}H NMR (400 MHz, DMSO-d_6, δ ppm): 7.79 (s, 1H), 7.65 (d, *J* = 8.0 Hz, 1H), 7.55 (s, 2H), 7.43 (d, *J* = 8.0 Hz, 1H), 7.19-7.16 (m, 1H), 7.09 (s, 1H), 7.06-7.03 (m, 1H), 6.96 (s, 1H), 6.84 (s, 1H, isoxazole), 5.10 (s, 2H, N-CH_2), 3.83 (s, 6H, 2×OCH_3), 3.53 (s, 3H, N-CH_3), 2.65 (s, 3H, -CH_3); ^{13}C NMR (100 MHz, DMSO-d_6, δ ppm): 169.57, 163.55, 161.35 (2C),

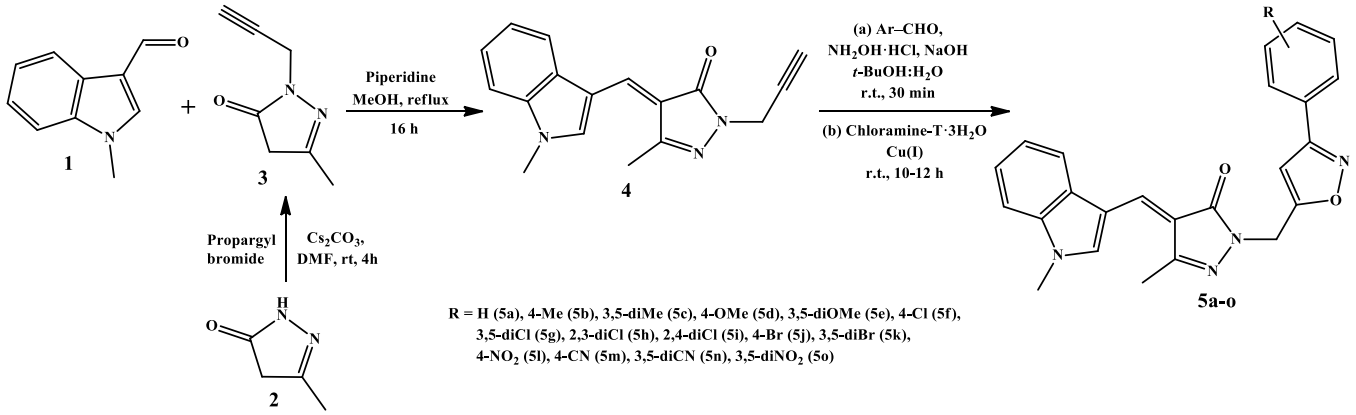

Scheme-I: Synthesis of indole–isoxazole–pyrazole hybrids (**5a-o**)

160.55, 154.27, 138.77, 134.25, 133.45, 132.50, 128.80, 124.41, 123.48, 122.39, 121.55, 117.43, 110.51, 108.25 (2C), 104.24, 99.85, 55.12 (2C), 44.21, 36.33, 14.82; ESI-MS: calcd. for $C_{26}H_{24}N_4O_4$: $[M]^+$ *m/z*: 456, found: 457 $[M+H]^+$. Anal. calcd. (found) % for $C_{26}H_{24}N_4O_4$: C, 68.41 (5.33); H, 5.30 (5.33); N, 12.27 (12.25).

(*E*)-2-((3-(4-Chlorophenyl)isoxazol-5-yl)methyl)-5-methyl-4-((1-methyl-1*H*-indol-3-yl)methylene)-2,4-dihydro-3*H*-pyrazol-3-one (5f): Yield: 63%; m.p.: 158-160 ºC; ^{1}H NMR (400 MHz, DMSO-d_6, δ ppm): 7.80 (s, 1H), 7.71 (d, *J* = 8.0 Hz, 2H), 7.65 (d, *J* = 8.0 Hz, 1H), 7.42 (d, *J* = 8.0 Hz, 1H), 7.33 (d, *J* = 8.0 Hz, 2H), 7.20-7.17 (m, 1H), 7.09 (s, 1H), 7.06-7.03 (m, 1H), 6.85 (s, 1H, isoxazole), 5.11 (s, 2H, N-CH_2), 3.52 (s, 3H, N-CH_3), 2.64 (s, 3H, -CH_3); ^{13}C NMR (100 MHz, DMSO-d_6, δ ppm): 169.21, 163.52, 160.29, 154.46, 138.97, 135.19, 133.39, 132.23, 129.03, 128.55 (2C), 127.90, 127.30 (2C), 124.23, 123.38, 122.11, 121.19, 117.56, 110.62, 99.76, 44.55, 36.61, 14.53; ESI-MS: Cal for $C_{24}H_{19}ClN_4O_2$: $[M]^+$ *m/z*: 430, found: 431 $[M+H]^+$. Anal. calcd. (found) % for $C_{24}H_{19}ClN_4O_2$: C, 66.90 (66.88); H, 4.44 (4.41); N, 13.00 (12.97).

(*E*)-2-((3-(3,5-Dichlorophenyl)isoxazol-5-yl)methyl)-5-methyl-4-((1-methyl-1*H*-indol-3-yl)methylene)-2,4-dihydro-3*H*-pyrazol-3-one (5g): Yield: 80%; m.p.: 150-152 ºC; ^{1}H NMR (400 MHz, DMSO-d_6, δ ppm): 7.80 (s, 1H), 7.73 (s, 2H), 7.63 (d, *J* = 8.0 Hz, 1H), 7.43 (d, *J* = 8.0 Hz, 1H), 7.29 (s, 1H), 7.20-7.17 (m, 1H), 7.09 (s, 1H), 7.06-7.03 (m, 1H), 6.88 (s, 1H, isoxazole), 5.11(s, 2H, N-CH_2), 3.53 (s, 3H, N-CH_3), 2.65 (s, 3H, -CH_3); ^{13}C NMR (100 MHz, DMSO-d_6, δ ppm): 169.72, 163.67, 160.36, 154.54, 138.77, 135.12 (2C), 133.86, 132.74, 130.85, 130.23, 128.44, 126.23 (2C), 124.68, 123.60, 122.53, 121.50, 117.61, 110.26, 99.74, 44.51, 36.23, 14.31; ESI-MS: calcd. for $C_{24}H_{18}Cl_2N_4O_2$: $[M]^+$ *m/z*: 464, found: 465 $[M+H]^+$. Anal. calcd. (found) % for $C_{24}H_{18}Cl_2N_4O_2$: C, 61.95 (61.91); H, 3.90 (3.87); N, 12.04 (12.01).

(*E*)-2-((3-(2,3-Dichlorophenyl)isoxazol-5-yl)methyl)-5-methyl-4-((1-methyl-1*H*-indol-3-yl)methylene)-2,4-dihydro-3*H*-pyrazol-3-one (5h): Yield: 43%; m.p.: 173-175 ºC; ^{1}H NMR (400 MHz, DMSO-d_6, δ ppm): 7.80 (s, 1H), 7.65 (d, *J* = 8.0 Hz, 1H), 7.57 (d, *J* = 8.0 Hz, 1H), 7.43 (d, *J* = 8.0 Hz, 1H), 7.34 (d, *J* = 8.0 Hz, 1H), 7.20-7.16 (m, 3H), 7.06-7.03 (m, 1H), 6.86 (s, 1H, isoxazole), 5.11(s, 2H, N-CH_2), 3.52 (s, 3H, N-CH_3), 2.65 (s, 3H, -CH_3); ^{13}C NMR (100 MHz, DMSO-d_6, δ ppm): 169.04, 163.37, 160.54, 154.53, 138.68, 133.70, 133.11, 132.64, 132.16, 131.45, 130.56, 128.29, 127.31, 127.07, 124.32, 123.29, 122.38, 121.60, 117.92, 110.74, 99.83, 44.19, 36.38, 14.72; ESI-MS: calcd. for $C_{24}H_{18}Cl_2N_4O_2$: $[M]^+$ *m/z*: 464, found: 465 $[M+H]^+$. Anal. calcd. (found) % for $C_{24}H_{18}Cl_2N_4O_2$: C, 61.95 (61.92); H, 3.90 (3.86); N, 12.04 (12.02).

(*E*)-2-((3-(2,4-Dichlorophenyl)isoxazol-5-yl)methyl)-5-methyl-4-((1-methyl-1*H*-indol-3-yl)methylene)-2,4-dihydro-3*H*-pyrazol-3-one (5i): Yield: 70%; m.p.: 169-171 ºC; ^{1}H NMR (400 MHz, DMSO-d_6, δ ppm): 7.80 (s, 1H), 7.63 (d, *J* = 8.0 Hz, 1H), 7.52 (d, *J* = 8.0 Hz, 1H), 7.42 (d, *J* = 8.0 Hz, 1H), 7.35 (s, 1H), 7.29 (d, *J* = 8.0 Hz, 1H), 7.21-7.18 (m, 1H), 7.09 (s, 1H), 7.05-7.02 (m, 1H), 6.86 (s, 1H, isoxazole), 5.11 (s, 2H, N-CH_2), 3.54 (s, 3H, N-CH_3), 2.64 (s, 3H, -CH_3); ^{13}C NMR (100 MHz, DMSO-d_6, δ ppm): 169.36, 163.88, 160.53, 154.27, 138.71, 136.34, 134.46, 133.32, 132.36, 131.36, 130.41, 129.35, 128.77, 127.26, 124.46, 123.52, 122.28, 121.56, 117.61, 110.22, 99.72, 44.60, 36.32, 14.82; ESI-MS: calcd. for $C_{24}H_{18}Cl_2N_4O_2$: $[M]^+$ *m/z*: 464, found: 465 $[M+H]^+$. Anal. calcd. (found) % for $C_{24}H_{18}Cl_2N_4O_2$: C, 61.95 (61.92); H, 3.90 (3.87); N, 12.04 (12.01).

(*E*)-2-((3-(4-Bromophenyl)isoxazol-5-yl)methyl)-5-methyl-4-((1-methyl-1*H*-indol-3-yl)methylene)-2,4-dihydro-3*H*-pyrazol-3-one (5j): Yield: 72%; m.p.: 172-174 ºC; ^{1}H NMR (400 MHz, DMSO-d_6, δ ppm): 7.80 (s, 1H), 7.64 (d, *J* = 8.0 Hz, 1H), 7.54-7.42 (m, 5H), 7.19-7.16 (m, 1H), 7.09 (s, 1H), 7.05-7.03 (m, 1H), 6.85 (s, 1H, isoxazole), 5.10 (s, 2H, N-CH_2), 3.53 (s, 3H, N-CH_3), 2.64 (s, 3H, -CH_3); ^{13}C NMR (100 MHz, DMSO-d_6, δ ppm): 169.61, 163.64, 160.41, 154.32, 138.76, 133.40, 132.68, 131.31 (2C), 128.71, 127.73, 126.73 (2C), 125.44, 124.32, 123.49, 122.57, 121.68, 117.59, 110.74, 99.84, 44.21, 36.27, 14.66; ESI-MS: calcd. for $C_{24}H_{19}BrN_4O_2$: $[M]^+$ *m/z*: 474, found: 475 $[M+H]^+$. Anal. calcd. (found) % for $C_{24}H_{19}BrN_4O_2$: C, 60.64 (60.66); H, 4.03 (4.00); N, 11.79 (11.76).

(*E*)-2-((3-(3,5-Dibromophenyl)isoxazol-5-yl)methyl)-5-methyl-4-((1-methyl-1*H*-indol-3-yl)methylene)-2,4-dihydro-3*H*-pyrazol-3-one (5k): Yield: 35%; m.p.: 181-183 ºC; ^{1}H NMR (400 MHz, DMSO-d_6, δ ppm): 7.79 (s, 1H), 7.66 (d, *J* = 8.0 Hz, 1H), 7.55 (s, 2H), 7.45 (d, *J* = 8.0 Hz, 1H), 7.35 (s, 1H), 7.20-7.16 (m, 1H), 7.09 (s, 1H), 7.05-7.02 (m, 1H), 6.85 (s, 1H, isoxazole), 5.11 (s, 2H, N-CH_2), 3.53 (s, 3H, N-CH_3), 2.64 (s, 3H, -CH_3); ^{13}C NMR (100 MHz, DMSO-d_6, δ ppm): 169.57, 163.75, 160.48, 154.44, 138.76, 135.13, 133.58, 132.52, 130.61, 128.74 (2C), 128.31, 125.38 (2C), 124.37, 123.32, 122.48, 121.19, 117.52, 110.32, 99.72, 44.31, 36.32, 14.76; ESI-MS: calcd. for $C_{24}H_{18}Br_2N_4O_2$: $[M]^+$ *m/z*: 552, found: 553 $[M+H]^+$. Anal. calcd. (found) % for $C_{24}H_{18}Br_2N_4O_2$: C, 52.01 (51.97); H, 3.27 (3.25); N, 10.11 (10.08).

(*E*)-5-Methyl-4-((1-methyl-1*H*-indol-3-yl)methylene)-2-((3-(4-nitrophenyl)isoxazol-5-yl)methyl)-2,4-dihydro-3*H*-pyrazol-3-one (5l): Yield: 77%; m.p.: 171-173 ºC; ^{1}H NMR (400 MHz, DMSO-d_6, δ ppm): 7.94 (d, *J* = 8.0 Hz, 2H), 7.79 (s, 1H), 7.63 (d, *J* = 8.0 Hz, 1H), 7.52 (d, *J* = 8.0 Hz, 2H), 7.43 (d, *J* = 8.0 Hz, 1H), 7.21-7.18 (m, 1H), 7.09 (s, 1H), 7.06-7.03 (m, 1H), 6.87 (s, 1H, isoxazole), 5.11 (s, 2H, N-CH_2), 3.53 (s, 3H, N-CH_3), 2.65 (s, 3H, -CH_3); ^{13}C NMR (100 MHz, DMSO-d_6, δ ppm): 169.48, 163.60, 160.28, 154.69, 149.05, 138.97, 135.08, 133.59, 132.46, 128.78, 127.71 (2C), 125.28 (2C), 124.60, 123.53, 122.71, 121.66, 117.65, 110.31, 99.86, 44.17, 36.29, 14.52; ESI-MS: calcd. for $C_{24}H_{19}N_5O_4$: $[M]^+$ *m/z*: 441, found: 442 $[M+H]^+$. Anal. calcd. (found) % for $C_{24}H_{19}N_5O_4$: C, 65.30 (65.27); H, 4.34 (4.31); N, 15.86 (15.83).

(*E*)-4-(5-((3-Methyl-4-((1-methyl-1*H*-indol-3-yl)methylene)-5-oxo-4,5-dihydro-1*H*-pyrazol-1-yl)methyl)isoxazol-3-yl)benzonitrile (5m): Yield: 44%; m.p.: 184-186 ºC; ^{1}H NMR (400 MHz, DMSO-d_6, δ ppm): 7.85 (d, *J* = 8.0 Hz, 2H), 7.79 (s, 1H), 7.64 (d, *J* = 8.0 Hz, 1H), 7.54 (d, *J* = 8.0 Hz, 2H), 7.44 (d, *J* = 8.0 Hz, 1H), 7.20-7.17 (m, 1H), 7.09 (s, 1H), 7.05-7.02 (m, 1H), 6.86 (s, 1H, isoxazole), 5.11 (s, 2H, N-CH_2), 3.53 (s, 3H, N-CH_3), 2.63 (s, 3H, -CH_3); ^{13}C NMR (100 MHz, DMSO-d_6, δ ppm): 169.61, 163.76, 160.54, 154.31, 138.71, 135.25, 133.59, 132.33 (2C), 131.33, 128.77 (2C), 127.18, 124.47, 123.34, 122.32, 121.44, 119.88, 117.59, 114.46, 110.23, 99.78,

44.82, 36.64, 14.52; ESI-MS: calcd. for $C_{25}H_{19}N_5O_2$: $[M+2H]^+$ *m/z* 421, found: 422 $[M+3H]^+$. Anal. calcd. (found) % for $C_{25}H_{19}N_5O_2$: C, 71.25 (71.23); H, 4.54 (4.51); N, 16.62 (16.59).

(*E*)-5-(5-((3-Methyl-4-((1-methyl-1*H*-indol-3-yl)methylene)-5-oxo-4,5-dihydro-1*H*-pyrazol-1-yl)methyl)isoxazol-3-yl)isophthalonitrile (5n): Yield: 54%; m.p.: 170-172 ºC; ^{1}H NMR (400 MHz, DMSO-d_6, δ ppm): 7.80 (s, 1H), 7.72 (s, 2H), 7.64 (d, *J* = 8.0 Hz, 1H), 7.49 (s, 1H), 7.42 (d, *J* = 8.0 Hz, 1H), 7.20-7.16 (m, 1H), 7.09 (s, 1H), 7.06-7.02 (m, 1H), 6.89 (s, 1H, isoxazole), 5.11(s, 2H, N-CH_2), 3.55 (s, 3H, N-CH_3), 2.65 (s, 3H, -CH_3); ^{13}C NMR (100 MHz, DMSO-d_6, δ ppm): 169.57, 163.52, 160.34, 154.44, 138.60, 136.03 (2C), 135.13, 133.45, 132.66, 131.23, 128.79, 124.67, 123.51, 122.78, 121.35, 118.14 (2C), 117.00, 116.19 (2C), 110.55, 99.82, 44.63, 36.36, 14.84; ESI-MS: calcd. for $C_{26}H_{18}N_6O_2$: $[M]^+$ *m/z*: 446, found: 447 $[M+H]^+$. Anal. calcd. (found) % for $C_{26}H_{18}N_6O_2$: C, 69.95 (69.97); H, 4.06 (69.97); N, 18.82 (18.78).

(*E*)-2-((3-(3,5-Dinitrophenyl)isoxazol-5-yl)methyl)-5-methyl-4-((1-methyl-1*H*-indol-3-yl)methylene)-2,4-dihydro-3*H*-pyrazol-3-one (5o): Yield: 38%; m.p.: 196-198 ºC; ^{1}H NMR (400 MHz, DMSO-d_6, δ ppm): 7.97 (s, 2H), 7.80 (s, 1H), 7.65 (d, *J* = 8.0 Hz, 1H), 7.61 (s, 1H), 7.42 (d, *J* = 8.0 Hz, 1H), 7.20-7.16 (m, 1H), 7.09 (s, 1H), 7.06-7.03 (m, 1H), 6.89 (s, 1H, isoxazole), 5.11 (s, 2H, N-CH_2), 3.54 (s, 3H, N-CH_3), 2.65 (s, 3H, -CH_3); ^{13}C NMR (100 MHz, DMSO-d_6, δ ppm): 169.64, 163.57, 160.47, 154.51, 146.23 (2C), 138.39, 133.65, 132.52, 131.57, 130.10 (2C), 128.27, 124.62, 123.60, 122.87, 122.42, 121.16, 117.46, 110.27, 99.76, 44.45, 36.53, 14.57; ESI-MS: calcd. for $C_{24}H_{18}N_6O_6$: $[M]^+$ *m/z*: 486, found: 487 $[M+H]^+$. Anal. calcd. (found) % for $C_{24}H_{18}N_6O_6$: C, 59.26 (59.23); H, 3.73 (3.70); N, 17.28 (17.32).

Determination of minimum inhibitory concentration (MIC): The MIC of the synthesized compounds was determined by the broth microdilution method according to the Clinical and Laboratory Standards Institute (CLSI) guidelines. Stock solutions of the synthesized compounds were prepared separately in DMSO and diluted with Mueller-Hinton broth (MHB; Becton Dickinson, Sparks, MD, USA) to obtain the required concentrations. Serial two-fold dilutions were prepared in 96-well microplates to obtain final concentrations ranging from 50 to 0.25 μg/mL. Fresh 24 h bacterial cultures were used for preparation of the inoculum. The bacterial suspension was adjusted to approximately 5×10^5 CFU/mL. An aliquot of 100 μL of the bacterial suspension was added to each well containing the respective concentration of the test compound. The plates were incubated at 37 ºC for 24 h. Following incubation, 40 μL of resazurin solution (0.4 μg/mL) was added to each well as a microbial growth indicator and the plates were further incubated at 37 ºC for 30 min. The MIC was recorded as the lowest concentration of the test compound at which no visible bacterial growth was observed. Appropriate growth and sterility controls were included in each assay. All experiments were performed in triplicate.

Growing of biofilm: The ability of the selected compounds to prevent biofilm development or destroy of preformed biofilms was investigated using a previously described method [31]. A 100 μL aliquot of standardized concentration of cultures with OD_{560} = 0.05 (5×10^3 CFU/mL) was added into individual flat-bottomed 96-well microtiter plates containing LB medium. The microtiter plate was incubated to develop a multilayer biofilm for approximately 24 h (irreversible attachment phase) and 48 h (mature biofilm) at 37 ºC. Following, different concentrations of the compounds (0-1000 μg/mL) were added into the wells of a 96-well microtiter plate and the plates were incubated further at 37 ºC for 24 h. Wells containing only media served as negative controls. Biofilm biomass was assessed using a crystal violet (CV) staining assay.

Crystal violet staining of biofilm: The crystal violet staining assay was performed as previously described, with minor modifications [32]. Following incubation, the contents of each well were removed by gently shaking and inverting the microtiter plate. The wells were then washed 3-4 times with sterile distilled water to remove loosely attached cells and residual culture medium. The plate was air-dried and subsequently dried in an oven at 60 ºC for 35-45 min. After drying, 125 μL of 0.1% (w/v) crystal violet solution was added to each well and incubated at room temperature for 10-15 min. The crystal violet solution was then removed and the wells were washed 4-5 times with sterile distilled water to remove excess dye. After washing, the biofilm appeared as a purple ring along the sidewalls of the wells. The plate was inverted and allowed to dry overnight before quantitative determination of the biofilm biomass. For quantitative analysis, the crystal violet retained by the biofilm was subsequently solubilized and the absorbance was measured using a microplate reader. The absorbance value was taken as an indicator of the amount of biofilm biomass present in each well.

RESULTS AND DISCUSSION

The synthetic sequence describes the synthesis of indole–isoxazole–pyrazole hybrids (**5a-o**) through sequential functionalization followed by Cu(I)-catalyzed 1,3-dipolar cycloaddition. Initially, 5-methyl-2,4-dihydro-3*H*-pyrazol-3-one (**2**) under-went base-promoted propargylation with propargyl bromide using Cs_2CO_3 in DMF at ambient temperature to afford the corresponding propargylated intermediate (**3**). Intermediate **3** was then subjected to Knoevenagel condensation with 1-methyl-1*H*-indole-3-carbaldehyde (**1**) in methanol under reflux in the presence of piperidine as a base catalyst. The active methylene group of the pyrazolone reacted with the aldehyde functionality to furnish the arylidene pyrazolone derivative (**4**). The resulting C=C bond remains conjugated with the carbonyl group, contributing to the stability of the intermediate. The key transformation involves the generation of nitrile oxides from substituted aromatic aldehydes. The aldehydes were treated with $NH_2OH{\cdot}HCl$ and NaOH in a butanol/water medium at ambient temperature to form the corresponding aldoximes. The oxidation of the aldoximes with chloramine-T trihydrate generated the reactive nitrile oxide species *in situ*. The nitrile oxide then underwent a Cu(I)-catalyzed regioselective [3+2] cycloaddition with the terminal alkyne moiety of compound **4** in THF at ambient temperature, affording the corresponding isoxazole ring. Cu(I) promotes formation of a copper acetylide from the terminal alkyne, which facilitates alkyne activation and directs the cycloaddition toward the observed regioisomer [33,34].

Antibacterial activity: The antibacterial efficacy of compounds **5a-o** was assessed against mutant strains of *S. aureus*:

methicillin-susceptible *S. aureus* (MSSA), methicillin-resistant *S. aureus* (MRSA) and vancomycin-resistant *S. aureus* (VRSA) using the conventional broth microdilution method [35]. The antibacterial data unequivocally indicate that the biological activity is significantly affected by the characteristics and placement of substituents on the aromatic ring (Table-1). The unsubstituted compound **5a** (R = H) was inactive (MIC > 50 μg/mL), affirming that substitution is crucial for antibacterial efficacy. Electron-donating groups such as 4-Me (**5b**) and 3,5-diMe (**5c**) exhibited only moderate activity, primarily against MRSA (25 μg/mL). Methoxy derivatives **5d** (4-OMe) and **5e** (3,5-diOMe) exhibited enhanced efficacy against MSSA (6.25-12.5 μg/mL), although they were less efficient against resistant strains. Halogen substitution markedly improved the antibacterial efficacy. The mono-chloro derivative **5f** (4-Cl) demonstrated considerable broad-spectrum efficacy (6.25-12.5 μg/mL). Notably, the dichloro derivatives exhibited superior efficacy, with **5g** (3,5-diCl) and **5i** (2,4-diCl) demonstrating exceptional potency against MSSA (1.56 μg/mL) and significant activity against MRSA and VRSA (3.12-6.25 μg/mL), comparable to dicloxacillin. Likewise, **5h** (2,3-dichlorophenyl) and **5k** (3,5-dibromophenyl) exhibited reliable and encouraging broad-spectrum inhibition within the 6.25 μg/mL range. Strong electron-withdrawing substituents, such as 4-NO_2 (**5l**) and 3,5-diNO_2 (**5o**), were associated with reduced activity (25-50 mg/mL), suggesting that excessive electron deficiency may be unfavorable for interactions with the target. Cyano derivatives **5m** (4-CN) and **5n** (3,5-diCN) exhibited moderate activity. The SAR demonstrates that dihalogen substitution, especially with chloro groups at the 3,5- or 2,4-positions, yields maximal antibacterial efficacy, presumably due to increased lipophilicity and advantageous interactions with bacterial targets. Among the disubstituted derivatives, dichloro derivatives exhibited potent activity then methoxy, cyano, bromo and nitro derivatives (Fig. 2).

The dichloro-substituted derivatives (**5g** and **5i**) exhibited superior antibacterial and antibiofilm activities, which may be associated with the combined electronic and lipophilic effects of the chlorine substituents. Chlorine acts as a moderately electron-withdrawing group while increasing the hydrophobic character of the molecule. The resulting enhancement in lipophilic surface area may promote penetration across the bacterial cell envelope and facilitate interactions with penicillin-binding proteins (PBPs). Molecular docking results supported this interpretation, with the 3,5- and 2,4-dichloro substitution patterns providing a suitable steric and electronic environment for hydrophobic and π-interactions with key amino acid residues within the binding site.

In contrast, strongly electron-withdrawing substituents such as nitro and cyano groups can substantially alter the electron distribution of the molecular framework, potentially affecting molecular recognition and target binding. The comparatively higher activity of **5g** and **5i** may, therefore, arise from a balance between electronic effects, lipophilicity, steric characteristics and favourable target interactions rather than from the presence of chlorine atoms alone.

TABLE-1
In vitro ANTIBACTERIAL ACTIVITY DATA FOR COMPOUNDS **5a-o**[a]

Compound	R	MIC (μg/mL)		
		MSSA	MRSA	VRSA
5a	H	>50	>50	>50
5b	4-Me	>50	25	>50
5c	3,5-diMe	12.5	25	>50
5d	4-OMe	12.5	25	50
5e	3,5-diOMe	6.25	25	50
5f	4-Cl	6.25	12.5	12.5
5g	3,5-diCl	1.56	1.56	6.25
5h	2,3-diCl	3.12	6.25	6.25
5i	2,4-diCl	1.56	3.12	6.25
5j	4-Br	25	50	50
5k	3,5-diBr	6.25	6.25	6.25
5l	4-NO_2	25	50	50
5m	4-CN	12.5	25	25
5n	3,5-diCN	25	12.5	12.5
5o	3,5-diNO_2	50	50	25
Dicloxacillin		3.12	6.25	6.25

"–" Indicates a concentration of > 50 μg/mL. [a]MIC *i.e.*, lowest concentration of the test compound required to inhibit bacterial growth.

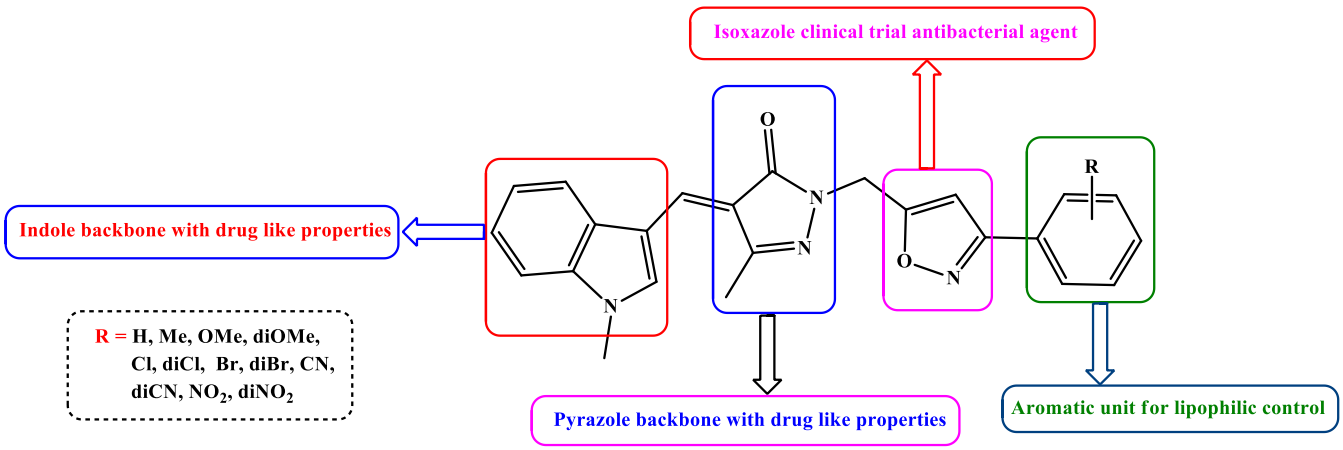

Fig. 2. SAR of the target fused 1,2,3-triazole derivatives

Antibiofilm activity: The MIC values identified several compounds with appreciable antibacterial activity, prompting their evaluation for antibiofilm efficacy (Table-2). Biofilm inhibition was assessed over a concentration range of 0-1000 μg/mL. Compounds **5f**, **5g**, **5h**, **5i** and **5k** exhibited significant biofilm inhibition, as reflected by their BFIC values in Table-2. Among these derivatives, **5i** (2,4-diCl) displayed the highest potency, with BFIC values of 3.89 μg/mL against MSSA, 5.52 μg/mL against MRSA and 12.89 μg/mL against VRSA. These values were comparable to those of dicloxacillin, which exhibited BFIC values of 4.39, 6.67 and 10.89 μg/mL, respectively. Compound **5g** (3,5-diCl) exhibited strong inhibition, with BFIC values ranging from 4.32 to 14.13 μg/mL, whereas **5h** (2,3-diCl) showed moderate activity. The mono-chloro derivative **5f** and the dibromo derivative **5k** exhibited comparatively weaker biofilm inhibition.

TABLE-2
BACTERIAL FILM INHIBITION CONCENTRATION (BFIC, μg/mL) OF COMPOUNDS **5f, 5g, 5h, 5i** AND **5k**

Bacteria	MSSA	MRSA	VRSA
5f	12.34**	16.33	23.33
5g	4.32***	8.69***	14.13**
5h	8.42**	11.32**	16.20
5i	3.89***	5.52***	12.89**
5k	15.13	22.53	28.43
Dicloxacillin	4.39	6.67	10.89

***$p < 0.001$, **$p < 0.05$.

The enhanced antibiofilm activity associated with the dichloro derivatives suggests that the position and number of halogen substituents play an important role in biological performance. The 2,4- and 3,5-dichloro substitution patterns may provide a favourable balance of electronic and lipophilic properties, which can facilitate interaction with bacterial biofilm associated targets and improve penetration into the biofilm matrix, particularly in resistant strains.

Correlation between MIC and BIC activities: The antibacterial and antibiofilm data demonstrated a distinct correlation, wherein drugs with reduced MIC values showed enhanced biofilm inhibition. Compound **5g** exhibited superior antibacterial activity (1.56-6.25 μg/mL) and a comparably robust antibiofilm effect (4.32-14.13 μg/mL), comparable to that of dicloxacillin. Compounds **5h** and **5i** exhibited moderate efficacy in both experiments, whereas **5f** and **5k**, with elevated MIC values, showed reduced biofilm inhibition. The higher planktonic antibacterial efficacy immediately facilitated improved biofilm formation avoidance.

Docking studies: The molecular interactions of compounds **5f**, **5g**, **5h**, **5i**, **5k** and dicloxacillin with the penicillin binding protein of *S. aureus* (MRSA) (PDB ID: 1 MWT, co-crystallized ligand inhibitor: Penicillin G were evaluated using *in silico* docking simulations [35]. Molecular docking demonstrated that all the synthesized compounds **5f-k** exhibited favourable binding inside the active site, with binding energies ranging from -6.76 to -7.17 kcal/mol. Compound **5h** had the highest affinity (-7.17 kcal/mol), comparable to that of penicillin G (-7.47 kcal/mol). The observed stability may be attributed to two hydrogen-bonding interactions with THR600 and ASN464, along with a π-anion interaction with GLU602 and a hydrophobic contact with TYR446. These interactions support a favourable orientation of the ligand within the binding pocket and may contribute to the stability of the ligand-target complex. Compounds **5k** and **5g** demonstrated robust binding *via* π-anion, π-lone pair and π-alkyl interactions despite the absence of traditional hydrogen bonds, underscoring the significance of hydrophobic stabilization. In contrast, compounds **5f** and **5i** exhibited modest affinities owing to restricted hydrogen bonding (Fig. 3). Dicloxacillin exhibited weaker binding despite forming several hydrogen bonds, which may be attributed to an unfavorable orientation within the binding pocket. The π-anion interaction with GLU602, together with a balanced network of hydrogen-bonding and hydrophobic interactions, appears to contribute to the favourable binding profile of **5h**. These interactions position **5h** as a promising lead for further structural optimization (Table-3).

Conclusion

Novel indole–pyrazole–isoxazole hybrids (**5a-o**) were synthesized, characterized and subjected to biological evalu-

TABLE-3
BINDING ENERGIES AND INTERACTIONS OF COMPOUNDS **5f**, **5g**, **5h**, **5i** AND **5k**

Compounds	Binding energy (Kcal mol^{-1})	Number of H-bonds	Key interactions
5f	-6.76	1	H-bond with **GLN521**, π-anion interaction with GLU602 and π-donor hydrogen bond interaction with ASN464.
5g	-6.98	–	The carbon hydrogen bond with SER462 and SER461, π--anion interaction with GLU602, π-lone pair with THR600 and π--alkyl interactions with THR446 and ALA642 were observed.
5h	-7.17	2	H-bond interactions with **THR600** and **ASN464**, π-anion interaction with GLU602 and π-alkyl interaction with TYR446.
5i	-6.78	1	H-bond interaction with **GLN521** and π–anion interactions with GLU602.
5k	-7.02	–	The carbon hydrogen bond with SER462 and SER461, π-anion interaction with GLU602, π-lone pair with THR600 and π-alkyl interactions with THR446 and ALA642.
Dicloxacillin	-6.27	4	H-bond interactions with **THR600, SER403** and **SER462**; Carbon hydrogen interaction with THR600; Sulfur interactions with MET641 and THR446; Pi-sigma with THR446; and Alkyl interaction MET641.
Penicillin G	-7.47	4	H-bond interactions with **SER403, ASN464** and **GLN521**; halogen interaction with THR444; unfavourable acceptor-acceptor interaction with SER462; Pi-anion with GLU602; Pi-Pi T-shaped with TYR446; alkyl interaction with ALA642.

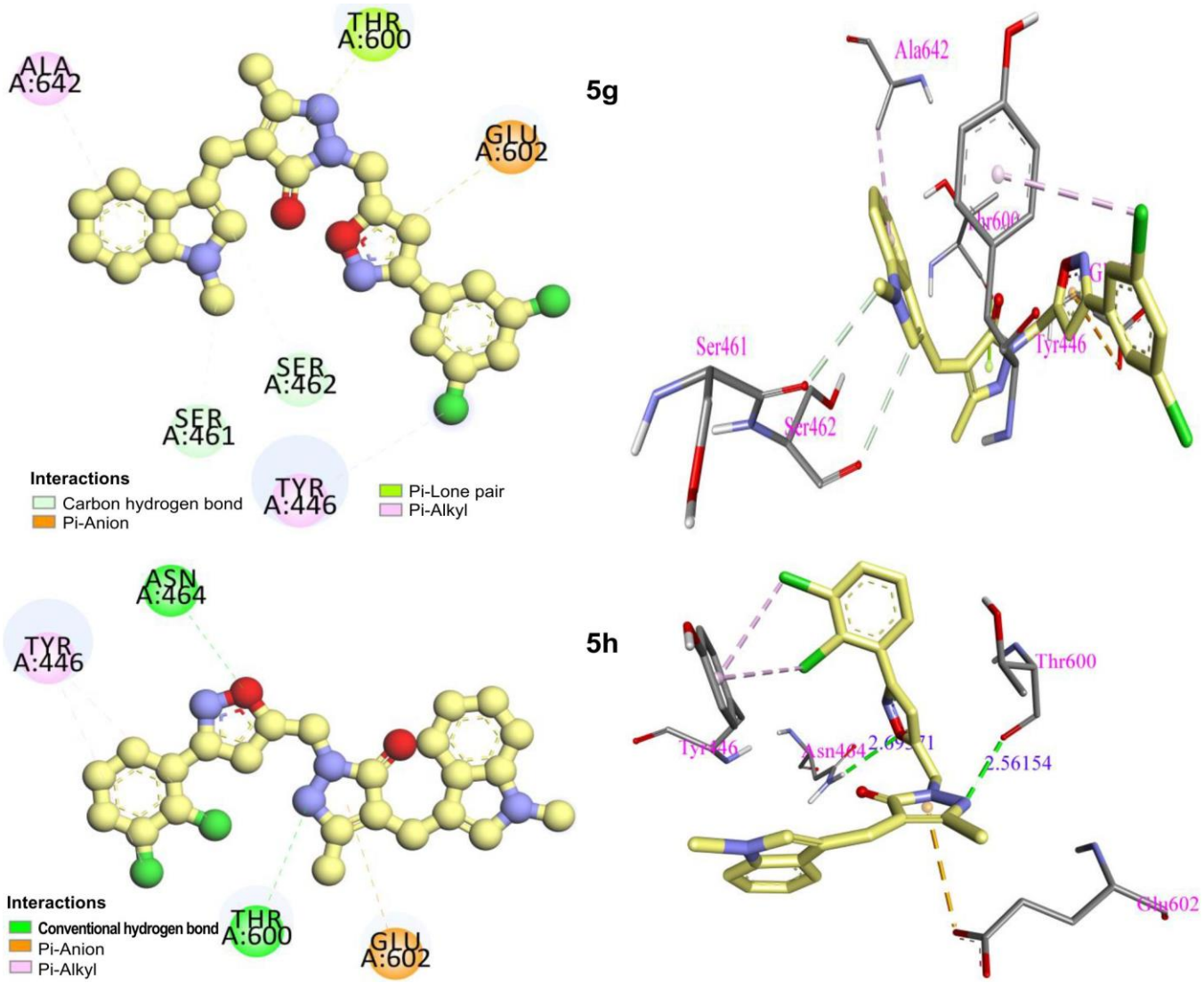

Fig. 3. 2D and 3D interactions of compounds **5g** and **5h** with penicillin-binding protein

ation. Dichloro-substituted derivatives, particularly **5g** and **5i**, exhibited pronounced antibacterial and antibiofilm activity against resistant *S. aureus* strains. Both compounds showed MIC values of 1.56 µg/mL against MSSA and MRSA and 6.25 µg/mL against VRSA. Compound **5i** displayed significant biofilm inhibition, with BFIC values ranging from 3.89 to 12.89 µg/mL, comparable to those of dicloxacillin. Molecular docking studies supported the *in vitro* results, with favourable interactions observed between the active compounds and the target protein. The structure-activity relationship analysis emphasized the importance of halogen substitution, particularly the dichloro pattern, in enhancing antibacterial and antibiofilm activity. These indole–pyrazole–isoxazole hybrids provide promising scaffolds for further structural optimization toward antibacterial agents active against multidrug resistant organisms.

CONFLICT OF INTEREST

The authors declare that there is no conflict of interests regarding the publication of this article.

DECLARATION OF AI-ASSISTED TECHNOLOGIES

During the preparation of this manuscript, the authors used an AI-assisted tool(s) to improve the language and no data, results or scientific conclusions were generated by AI. All analyses, interpretations and conclusions are the authors' own. The authors reviewed and edited the content and take full responsibility for the published work.

REFERENCES

1. C.P. Pandhurnekar, H.C. Pandhurnekar, A.J. Mungole, S.S. Butoliya and B.G. Yadao, *J. Heterocycl. Chem.*, **60**, 537 (2023); https://doi.org/10.1002/jhet.4586.
2. G.J. Martis and S.L. Gaonkar, *RSC Adv.* **15**, 8213 (2025); https://doi.org/10.1039/d4ra08339c
3. Y.R. Girish, K.S.S. Kumar, H.S. Manasa and S. Shashikanth, *J. Chin. Chem. Soc.*, **61**, 1175 (2014); https://doi.org/10.1002/jccs.201400170
4. T.R. Swaroop, K.S. Sharath Kumar, M. Palanivelu, S. Chaitanya and K.S. Rangappa, *J. Heterocycl. Chem.*, **51**, 1866 (2014); https://doi.org/10.1002/jhet.1864

5. H. Ananda, K.S. Sharath Kumar, M. Nishana, M. Srivastava, M. Hegde, R. Byregowda, B. Choudhary, S.C. Raghavan and K.S. Rangappa, *Mol. Cell. Biochem.*, **426**, 149 (2017); https://doi.org/10.1007/s11010-016-2887-7
6. H.R. Puneeth, H. Ananda, K.S.S. Kumar, K.S. Rangappa and A.C.S. Sharada, *Med. Chem. Res.*, **25**, 1842 (2016); https://doi.org/10.1007/s00044-016-1628-5
7. S. Michael Marcy and J.O. Klein, *Med. Clin. North Am.*, **54**, 1127 (1970); https://doi.org/10.1016/S0025-7125(16)32582-2
8. R.A. Al-Qawasmeh, M. Huesca, V. Nedunuri, R. Peralta, J. Wright, Y. Lee and A. Young, *Bioorg. Med. Chem. Lett.*, **20**, 3518 (2010); https://doi.org/10.1016/j.bmcl.2010.04.137
9. A. Kumari and R.K. Singh, *Bioorg. Chem.*, **89**, 103021 (2019); https://doi.org/10.1016/j.bioorg.2019.103021
10. F. Song, Z. Li, Y. Bian, X. Huo, J. Fang, L. Shao and M. Zhou, *Arch. Pharm.*, **353**, e2000143 (2020); https://doi.org/10.1002/ardp.202000143
11. T. Meng, Y. Hou, C. Shang, J. Zhang and B. Zhang, *Arch. Pharm.*, **354**, e2000266 (2021); https://doi.org/10.1002/ardp.202000266
12. F. Gao, L. Ye, F. Kong, G. Huang and J. Xiao, *Bioorg. Chem.*, **91**, 103162 (2019); https://doi.org/10.1016/j.bioorg.2019.103162
13. V.P. Kumar, J. Renjitha, C.T. Fathimath Salfeena, K.T. Ashitha, S.K. Rangappa, V. Sunil and B.S. Sasidhar, *Chem. Biol. Drug Des.*, **90**, 703 (2017); https://doi.org/10.1111/cbdd.12990
14. S. Narsimha, N.S. Kumar, B.K. Swamy, N.V. Reddy, S.K. Althaf Hussain and M.S. Rao, *Bioorg. Med. Chem. Lett.*, **26**, 1639 (2016); https://doi.org/10.1016/j.bmcl.2016.01.055
15. K. Lewis, *Cell*, **181**, 29 (2020); https://doi.org/10.1016/j.cell.2020.02.056
16. H.F. Wertheim, M.C. Vos, A. Ott, A. van Belkum, A. Voss, J.A.J.W. Kluytmans, P.H.J. van Keulen, C.M.J.E. Vandenbroucke-Grauls, M.H.M. Meester and H.A. Verbrugh, *Lancet*, **364**, 703 (2004); https://doi.org/10.1016/S0140-6736(04)16897-9
17. T.E. Kehl-Fie, Y. Zhang, J.L. Moore, A.J. Farrand, M.I. Hood, S. Rathi, W.J. Chazin, R.M. Caprioli and E.P. Skaar, *Infect. Immun.*, **81**, 3395 (2013); https://doi.org/10.1128/IAI.00420-13
18. N. Chandal, R. Kalia, A. Dey, R. Tambat, N. Mahey, S. Jachak and H. Nandanwar, *Commun. Biol.*, **7**, 1489 (2024); https://doi.org/10.1038/s42003-024-06996-8
19. N. Ramu, T.M. Krishna, R. Kapavarapu and S. Narsimha, *RSC Adv.*, **14**, 8921 (2024); https://doi.org/10.1039/D3RA07509E
20. Y. Jia, W. Chen, R. Tang, J. Zhang, X. Liu, R. Dong, F. Hu and X. Jiang, *Cell Host Microbe*, **31**, 1101 (2023); https://doi.org/10.1016/j.chom.2023.06.008
21. D. Carcione, J. Intra, L. Andriani, F. Campanile, F. Gon, S. Carletti, N. Mancini, G. Brigante, D. Cattaneo, S. Baldelli, M. Chisari, A. Piccirilli, S. Di Bella and L. Principe, *Pharmaceuticals*, **16**, 1304 (2023); https://doi.org/10.3390/ph16091304
22. H. Brüssow, *Microb. Biotechnol.*, **17**, e14510 (2024); https://doi.org/10.1111/1751-7915.14510
23. M.H. Muhammad, A.L. Idris, X. Fan, Y. Guo, Y. Yu, X. Jin, J. Qiu, X. Guan and T. Huang, *Front. Microbiol.*, **11**, 928 (2020); https://doi.org/10.3389/fmicb.2020.00928
24. K. Sauer, P. Stoodley, D.M. Goeres, L. Hall-Stoodley, M. Burmølle, P.S. Stewart and T. Bjarnsholt, *Nat. Rev. Microbiol.*, **20**, 608 (2022); https://doi.org/10.1038/s41579-022-00767-0
25. A. Ali, A. Zahra, M. Kamthan, F.M. Husain, T. Albalawi, M. Zubair, R. Alatawy, M. Abid and M.S. Noorani, *Microorganisms*, **11**, 1934 (2023); https://doi.org/10.3390/microorganisms11081934
26. H. Parveen, S. Mukhtar, M.O. Albalawi, S. Khasim, A. Ahmad and M.Y. Wani, *Pharmaceutics*, **16**, 1570 (2024); https://doi.org/10.3390/pharmaceutics16121570
27. K. Qvortrup, L.D. Hultqvist, M. Nilsson, T.H. Jakobsen, C.U. Jansen, J. Uhd, J.B. Andersen, T.E. Nielsen, M. Givskov and T. Tolker-Nielsen, *Front. Chem.*, **7**, 742 (2019); https://doi.org/10.3389/fchem.2019.00742
28. M.D. Bandgar, S. Peddapelli, R. Kapavarapu, J. Boruwa, S. Kavela and S. Narsimha, *RSC Med. Chem.*, **16**, 4154 (2025); https://doi.org/10.1039/D5MD00103J
29. N. Ramu, T.M. Krishna, V. Nasipireddy, R. Kapavarapu and S. Narsimha, *ChemistrySelect*, **8**, e202300777 (2023); https://doi.org/10.1002/slct.202300777
30. E. Ramya Sucharitha, T.M. Krishna, R. Manchal, G. Ramesh and S. Narsimha, *Bioorg. Med. Chem. Lett.*, **47**, 128201 (2021); https://doi.org/10.1016/j.bmcl.2021.128201
31. E.F. Haney, M.J. Trimble and R.E.W. Hancock, *Nature Protocols*, **16**, 2615 (2021); https://doi.org/1038/s41596-021-00515-3
32. S. Stepanović, D. Vuković, V. Holá, G. Di Bonaventura, S. Djukić, I. Ćirković and F. Ruzicka, *APMIS*, **115**, 891 (2007); https://doi.org/10.1111/j.1600-0463.2007.apm_630.x
33. T.V. Hansen, P. Wu and V.V. Fokin, *J. Org. Chem.*, **70**, 7761 (2005); https://doi.org/10.1021/jo050163b
34. M.D.A.A. Pasha, E.R. Sucharitha, R. Kapavarapu, S. Narsimha, A. Dubba and K. Siddoju, *ChemistrySelect*, **10**, e202504361 (2025); https://doi.org/10.1002/slct.202504361
35. K. Premalatha, R. Kapavarapu, S.I. Al-Resayes, V. Nasipireddy, M. Azam, and S. Narsimha, *ChemistrySelect*, **9**, e202401858 (2024); https://doi.org/10.1002/slct.202401858